Evaluation of Dutch backward erosion piping models and a future perspective

V.M. van Beek & G.J.C.M. Hoffmans
Deltares

Abstract: The prediction of backward erosion piping is important for safety assessment of dikes in the Netherlands, where subsurface conditions are prone to this erosion mechanism. In the current assessment methodology, the adapted Sellmeijer rule is in use. In combination with the national safety philosophy and uncertainty in input parameters, this model results in high failure probabilities. This paper evaluates the Sellmeijer model and the recently developed Shields-Darcy model alongside recent developments in research on modelling of backward erosion piping, leading to a future perspective.

Keywords: Backward erosion piping, Shields-Darcy model, Sellmeijer model, groundwater flow, incipient motion.

1 INTRODUCTION

Backward erosion piping is a failure mechanism for dams and dikes whereby particles are transported from granular layers under the action of water flow, leaving a shallow hollow space (a pipe), which progressively develops in the opposite direction of water flow. Given enough time and sufficient hydraulic loads, the process will eventually lead to undermining and breach of the water-retaining structure.

The process typically occurs in granular and relatively uniform layers covered by a cohesive layer that forms a roof to the pipe. This situation is often found in deltaic and fluvial areas. Given an unfiltered exit to the surface and a sufficient head drop across the structure, transported sand accumulates in a ring around the downstream defect, forming a sand boil. Sand boils are often observed during high waters, for example along some of the main rivers in the Netherlands, United States, Italy and China.

In the Netherlands, a few dike failures are attributed to backward erosion piping (Vrijling et al., 2010). More recent case histories are known in the United States, such as Kaskaskia Island and Bois Brule (Navin, 2016). The excessive number of sand boils observed during high water in relation to the relatively small number of failure cases is one of the indicators that optimized prediction of failure should be related to the prediction of the development of the pipe towards the upstream side rather than to the prediction of initial sand boil formation. Experiments at a small and medium scale confirm that sand boils can form at lower water levels than required for pipes to progress towards the upstream side, eventually leading to failure (Van Beek et al., 2015).

Safety assessment in the Netherlands for backward erosion piping consists of a multi-staged approach. The first step (elementary assessment) consists of a set of simple rules to judge the possibility of backward erosion piping for a certain dike section. Dikes that fail this elementary assessment are subjected to a detailed assessment, in which the failure probability is determined for the processes of uplift of the cover layer, transport of particles through a defect (heave) and the progression of the pipe. The uplift calculation is based on the comparison of water pressures in the aquifer and the overlying weight of the blanket layer. For the vertical transport of particles through the defect a critical vertical gradient of 0.3 across the blanket layer is used. The probability for pipe progression is calculated using the Sellmeijer rule (Sellmeijer et al., 2011). The final step in the safety assessment consists of a tailormade analysis using more detailed data or software, for example DGFlow (Van Esch et al., 2013) in which the Sellmeijer model is implemented.

Due to several changes in the backward erosion safety assessment in the recent years, such as the inclusion of the length effect (investigated by Kanning (2012)), the transition from dikes regulated by the probability of a flood level to a probability of flooding per section of each dike ring (Vrijling et al., 2011b), the abandoning of Bligh's rule (Bligh, 1910) and an adjustment in the Sellmeijer rule (Sellmeijer et al., 2011), more dike sections fail the new (detailed) assessment. Therefore, a need exists for more advanced piping prediction. This challenge is faced by several research groups around the world. In the past years new insights have been developed, both in experimental and numerical aspects. Parallel to the various laboratory and numerical efforts to understand and simulate the backward erosion process, Hoffmans (2014) has developed a method for prediction of pipe progression, the Shields-Darcy (SD) model.

This paper presents the similarities and differences of the two currently available Dutch backward erosion piping models (the Sellmeijer model and the SD model) alongside with new insights into backward erosion piping, leading to a future perspective of backward erosion modeling.

2 EVALUATION OF DUTCH BACKWARD EROSION PIPING MODELS

The Sellmeijer model and the SD model have many similarities. Both models attempt to predict the critical head at which the pipe progresses towards the upstream side by analyzing the groundwater flow towards the pipe, the flow through the pipe, and erosion criteria for onset of particle motion.

2.1 Groundwater flow

It is clear that groundwater flow is the driving force for the occurrence of backward erosion piping. In the early days of piping prediction (Bligh, 1910; Lane (1935), many people already stressed the importance of modelling groundwater flow (Harza, 1935, Terzaghi in response to Lane (1935)). It has been demonstrated by various researchers that the effect of scale (represented by seepage length or aquifer depth) on the overall critical gradient can be explained by groundwater flow (Sellmeijer et al., 1989, De Wit, 1984, Van Beek et al., 2014). The critical gradient decreases with increase of scale, which is related to the larger area available for flow.

Initially the Sellmeijer model was developed with analytical equations for 2D groundwater flow towards the pipe (Sellmeijer, 1988) for an infinitely deep aquifer. The limited application of such a model was soon realized, resulting in a mathematical formulation of groundwater flow towards the pipe in homogeneous and isotropic aquifers with finite depth (Sellmeijer et al., 1989). The Sellmeijer model was implemented in the 2D groundwater finite element model MSEEP, in which the pipe was modelled as a boundary condition with the head at the boundary based on equations for pipe flow and limit state equilibrium of particles (Sellmeijer, 2006). In this way numerical calculations could be used for determining the flow towards the pipe, allowing for more complex (multi-layer and anisotropic) subsurface configurations. The rule currently used in the safety assessment (Sellmeijer et al., 2011) is a curve-fit based on thousands of piping calculations in MSEEP. Recently the model has been implemented in DGFlow, a more refined FEM allowing for transient flow (Van Esch et al., 2013), using one-dimensional line elements.

The SD model (Hoffmans, 2014) approximates the 2D groundwater flow towards the pipe for a homogeneous and isotropic sand layer. The groundwater flow is schematized by defining two zones (see Figure 1): Zone A with thickness D_{ref} close to the pipe (where there is a dip in the hydraulic gradient) and Zone B at greater depth (where the hydraulic head is assumed not to be affected by the flow towards the pipe). It is assumed that the flow through Zone B does not affect the piping mechanism at all.

The thicknesses of zone A and B are not defined directly, but the concept of divided flows is used in the derivation of equations. The derived thickness of Zone A is discussed in section 2.4. Next to this, it is assumed that the flow upstream of the pipe is horizontal, and thus that the gradient upstream of the pipe is constant. In the influence zone of the pipe (in Zone A, below the pipe), the flow towards the pipe is calculated, assuming a linear head drop in the pipe for reasons of simplicity. It is assumed that all of the water flowing through Zone A flows towards the pipe (implying that no water flows out of zone A). This leads to equation 1, describing the critical average gradient across the structure, which, when exceeded will lead to ongoing pipe formation. The average critical gradient was based on the critical pipe length ℓ_c the critical pipe gradient (at which the particles are in limit-state equilibrium) and the critical gradient in the zone upstream of the pipe, which is based on the distribution of flow towards the pipe and the resistance of the pipe (see section 2.4).

$$\frac{H_c}{L} = S_{pipe,c} + \left(1 - \frac{\ell_c}{L}\right)\left(S_{sand,c} - S_{pipe,c}\right) \tag{1}$$

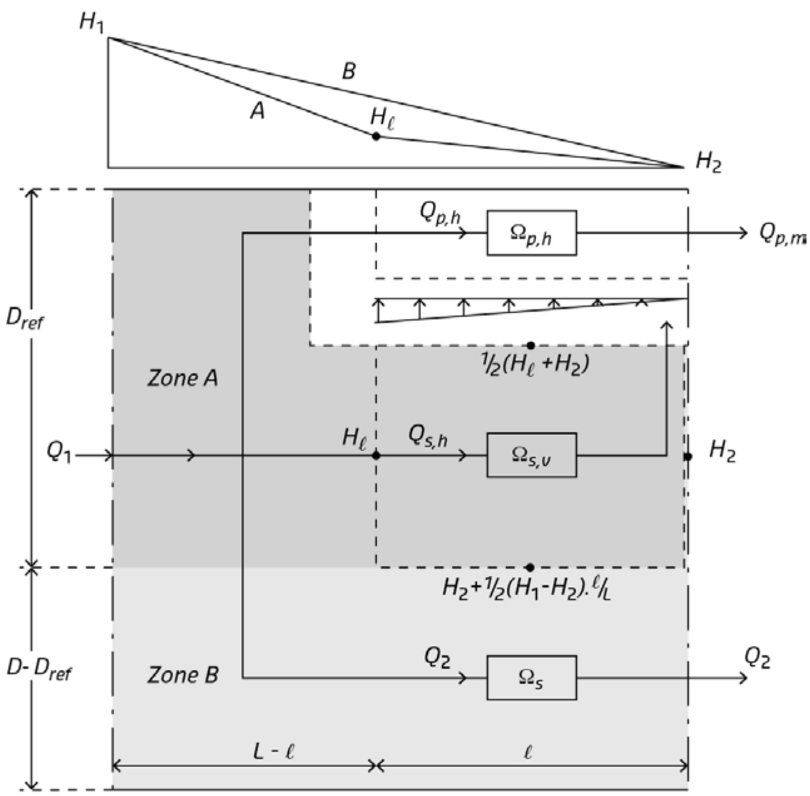

Figure 1. Resistance schematization in sand layer in the SD-model

New insights focus on the value of more detailed analysis of groundwater flow. Although the groundwater flow was examined quite accurately in MSEEP for 2D situations already, Vandenboer et al. (2014a) and Van Beek et al. (2015) illustrated that the difference in critical head between 3D flow towards a single point exit as opposed to a 2D exit (like a ditch or outflow area) is large, in experiments about a factor of 2, causing predictions based on 2D calculations to be unsafe. Vandenboer et al. (2014b) investigated the effect of the third dimension by varying the width of the experimental configuration. From multi-layer piping experiments conducted by Müller-Kirchenbauer (1978), Ding et al. (2007) and Van Beek et al. (2012), it can be concluded that schematizing the subsurface with one homogeneous layer does not result in optimized predictions, but may serve as a first approximate if the permeability is conservatively chosen. First attempts have now been made to model the piping process in 3D (Vandenboer et al. (2014a), Robbins (2016), Van Esch et al. (2013), Rotunno et al. (2017)).

The assumption of steady state flow, generally valid for laboratory experiments, is expected to be conservative in the field, where both the hydraulic load and the response in the aquifer are time-dependent. To account for this effect, the Sellmeijer model has been implemented in the finite element model DGFlow (Van Esch et al., 2013), allowing for transient groundwater flow.

2.2 Pipe flow

Both the Sellmeijer model and SD model use equations for laminar and incompressible flow in the pipe to assess the load on the particles in the pipe. Sellmeijer continues the 2D approach applied for groundwater flow and assumes pipes of infinite width. For this situation Sellmeijer (1988) solved the Navier-Stokes equations, resulting in the Hagen-Poiseuille equation for parallel plates:

$$\rho g \frac{d\varphi}{dx} a^3 = 12 q \mu \tag{2}$$

in which a is the pipe height. Hoffmans (2014) uses an equation for circular pipes with the hydraulic radius, applicable for different shapes, for which the equation holds:

$$\pi \rho g S_{pipe} N R^4 = \tfrac{1}{2} \mu Q \tag{3}$$

in which R is the hydraulic radius of the pipe. The total flow is multiplied by N, representing the number of pipes. The load acting on the particles on the pipe bottom is represented by the wall shear stress, defined as below for infinitely wide pipes (approach Sellmeijer) and pipes with hydraulic radius R (SD-model) respectively:

$$\tau_w = \frac{a}{2} \rho g \frac{d\varphi}{dx} \tag{4}$$

and

$$\tau_w = R \rho g S_{pipe} \tag{5}$$

The pipe shape is relevant in connecting the flow and head loss in the pipe to a shear stress. Measurements in experiments (Hanses, 1985 and Van Beek et al., 2015) indicate that the pipe is relatively shallow compared to its depth. Ratios of width and depth were analysed by Van Beek (2015) and were found to be in the order of 7-13 for two analysed different sand types, i.e. such that the assumption of the equation for parallel plates is justified. The consequences of using equations with a hydraulic radius rather than with a flat wide pipe is not investigated here, but the parallel plates seem a more obvious choice in future considerations.

The assumption of laminar flow is most likely valid for fine to medium sands (Robbins and Van Beek, 2017), but may not be suited for all sand types encountered. More research is required to investigate the effect of wall turbulence and turbulent flow in the pipe on backward erosion piping.

2.3 Erosion criteria

To determine whether a pipe can or cannot progress, erosion criteria need to be defined. Hanses (1985) defined two types of erosion relevant for pipe progression: erosion at the pipe tip, causing the pipe to lengthen and referred to as primary erosion, and erosion of the pipe walls and bottom, deepening and widening the pipe, referred to as secondary erosion.

Both the Sellmeijer model and the SD model rely on secondary erosion only, and thus base the pipe progression on the critical conditions in the pipe. In the Sellmeijer model the pipe is assumed to be in equilibrium when the particles at the pipe bottom are in equilibrium at every location in the pipe. When this equilibrium is exceeded, the pipe is assumed to lengthen.

In the previous section the shear stress exerted by the water on the particles is described for the situation of an infinitely wide pipe. The limit-state equilibrium is defined in the Sellmeijer model by defining a critical shear stress according to White (1940), who considered the equilibrium of forces on the particles in relation to the distribution of the load over a group of particles:

$$\tau_c = \eta \frac{\pi}{6} \gamma_p' d \tan\theta \tag{6}$$

In which η is the coefficient of White and θ is the bedding angle (rolling resistance in top layer of grains). In White's approach the coefficient η was originally combined with another coefficient α, the former describing the ratio of the area of the grains over which the shear stress is divided to the total area considered, the latter being an experimental coefficient to account for the action of forces above the gravity of the grain. The combined coefficient of αη was later simplified by Sellmeijer to η. Based on the flume experiments on two sand types in which White studied the incipience of motion in laminar flow, Sellmeijer defined a constant and conservative (compared to the values suggested by White) value of 0.25 for the coefficient of White. The bedding angle, also derived by White in two experiments, was used later as a calibration parameter in large scale backward erosion piping experiments (described later on in the section on calibration) and applied as a constant in the current assessment rule. The particle diameter, *d*, was not described in detail by White, but Sellmeijer (1988) assumed that the representative particle size should be between d_{65} and d_{75} since fine particles are more easily transferred than larger particles, and larger particles need to be transported as well. In later publications the d_{70} was chosen as the representative grain diameter (TAW, 1999, Sellmeijer et al., 2011).

In the SD model the pipe lengthens, widens and deepens when the average gradient in the pipe exceeds a critical value (S_{pipe}>$S_{pipe,c}$). The progression is therefore determined by the equilibrium of particles in the pipe (secondary erosion), rather than by a criterion for loosening and detaching the intact sand bed upfront of the pipe (primary erosion). Hoffmans (2014) was the first to apply the Shields diagram (1936) for incipient motion to backward erosion piping. In this approach the threshold of particle movement is governed by balancing the driving force and the resistance force, similarly to the approach by White, but by lumping the unknown coefficients into one parameter, the critical Shields parameter:

$$\tau_c = \Psi_c \gamma_p' d_{50} \tag{7}$$

The Shields parameter is determined using many flume experiments, both in turbulent and laminar flow, and was found to be a function of the Reynolds shear number. Due to the pressure fluctuations typical for turbulent flow, particles move easier in turbulent flow than in laminar flow. Since the flow in the pipes is assumed to be laminar, Hoffmans (2014) proposed a relation for estimating the critical shear stress, based on the laminar flow flume experiments by Govers (1987), Pilotti and Menduni (2001) and Loiseleux et al. (2005), in the range of 0.1 mm<d_{50}<0.5 mm:

$$\Psi_c = 0.2\left(D_*\right)^{-1/3} \text{ for } 2 \le D_* \le 15 \tag{8}$$

in which D_* is the dimensionless particle number:

$$D_* = d_{50}\left(\frac{\Delta g}{\nu^2}\right)^{1/3} \tag{9}$$

Although the critical Shields parameters were determined based on the d_{50} (equation 7), Hoffmans and Van Rijn (2017) proposed to use the d_{15} instead of the d_{50} to account for grading in the sand, since according to the load and strength probability distributions proposed by Grass (1970), the finer particles will move first for sands with d_{90}/d_{10} under 4:

$$\tau_{c,k} = \Psi_c \gamma_p' d_{15} \tag{10}$$

The approach by Grass was developed for turbulent flow and it is yet unclear whether it is also applicable to laminar flow. The use of a median particle diameter could be advocated based on the observations by

Govers (1987), who found that in laminar flow particles tend to move as a grain carpet, giving a sharply discernible critical state for incipient motion, due to the lack of fluctuating shear stresses typical for turbulent flow.

For graded sands with d_{90}/d_{10}>4, the finer particles are not representative for describing the initiation of motion as they could be locked between the coarser ones (Van Rijn, 2014). In such cases it is recommended to use d_{50}, or an upper limit, for example d_{70}. It is noted that equation 9 was not altered with respect to the representative grain size.

Recent research suggests (Robbins and Van Beek, 2017) that the Shields approach, applied with d_{50} as representative diameter, is reasonable for the prediction of the gradient in the pipe. The use of a constant bedding angle in the approach by White causes an overestimation of the critical gradient, unless this is corrected for in other parameters (as is done in the adapted rule in Sellmeijer et al., 2011). More research is required to understand the incipient motion of particles for the specific conditions of shallow pipes in sands of variable density.

Recent developments focus not only on criteria for secondary erosion, but also on criteria for primary erosion. Several authors agree that a local scale-independent criterion exists that causes the progression of the pipe (Hanses, 1985, Van Beek et al., 2015, Robbins et al., t.b.p., Rotunno et al., 2017). An important aspect is that this is a *local* phenomenon: the velocities and gradient upstream of the pipe locally rise due to the concentration of flow. This was well illustrated by De Wit (1984) using Figure 2, which shows the head drop below an impervious structure, with identical local gradients near the exit, but varying average gradients for two scales. A similar figure could be drawn for the situation with a pipe. Even when a criterion for primary erosion would control the progression, secondary erosion affects the head loss in the pipe and therefore indirectly influences the local gradient upstream of the pipe.

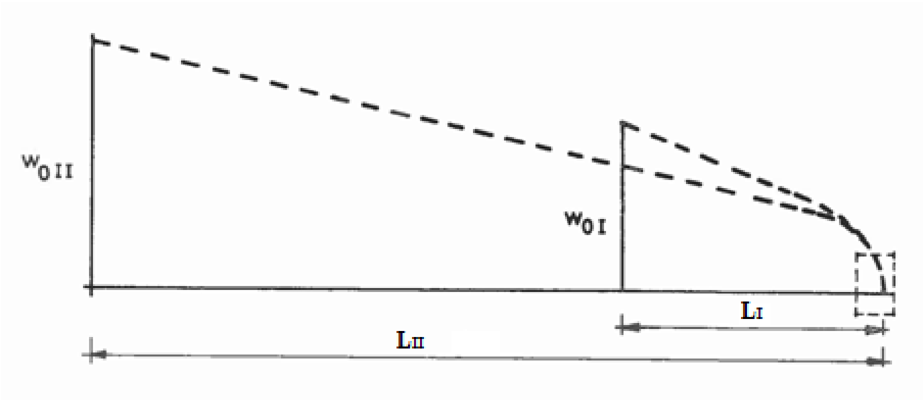

Figure 2: Head distribution in critical conditions (critical head drop denoted by w_0) in two identical set ups, but with different seepage lengths. Identical local gradients, but varying overall gradients below impervious structures of different sizes (adapted after De Wit, 1984)

2.4 Synthesis

Originally the Sellmeijer model combined the analytical equations for groundwater flow to the equations for pipe flow and particle equilibrium to find an 'equilibrium head' for each pipe length. Later (Sellmeijer, 2006) numerical groundwater calculations were conducted to solve the specific boundary conditions and to find the equilibrium head at different pipe lengths. The maximum equilibrium head found in this way is denoted as the critical head. The specific boundary condition which is solved is obtained by combining equations 2, 4 and 6, eliminating the pipe height, and reads:

$$Q\left(\frac{d\varphi}{dx}\right)^2 = \frac{\gamma_w}{12\mu}\left(\frac{\pi}{3}\frac{\gamma_p'}{\gamma_w}d\eta\tan\theta\right)^3 \tag{11}$$

By curve-fitting and comparison with a very large number of numerical calculations in MSEEP a relation was obtained between the critical head and the material properties, for a standard dike geometry which agrees very well with the numerical results and which reads (Sellmeijer et al., 2011):

$$\frac{H_c}{L} = F_R F_S F_G \qquad \begin{aligned} F_R &= \eta \frac{\gamma_p'}{\gamma_w} \tan\theta \\ F_S &= \frac{d_{70}}{\sqrt[3]{\kappa L}} \\ F_G &= 0.91 \left(\frac{D}{L}\right)^{\frac{0.28}{\left(\frac{D}{L}\right)^{2.8} - 1} + 0.04} \end{aligned} \tag{12}$$

The SD model is synthesized starting with the simplified equation for groundwater flow (equation 1, variables illustrated in figure 3).

$$\frac{H_c}{L} = S_{pipe,c} + \left(1 - \frac{\ell_c}{L}\right)\left(S_{sand,c} - S_{pipe,c}\right) \tag{13}$$

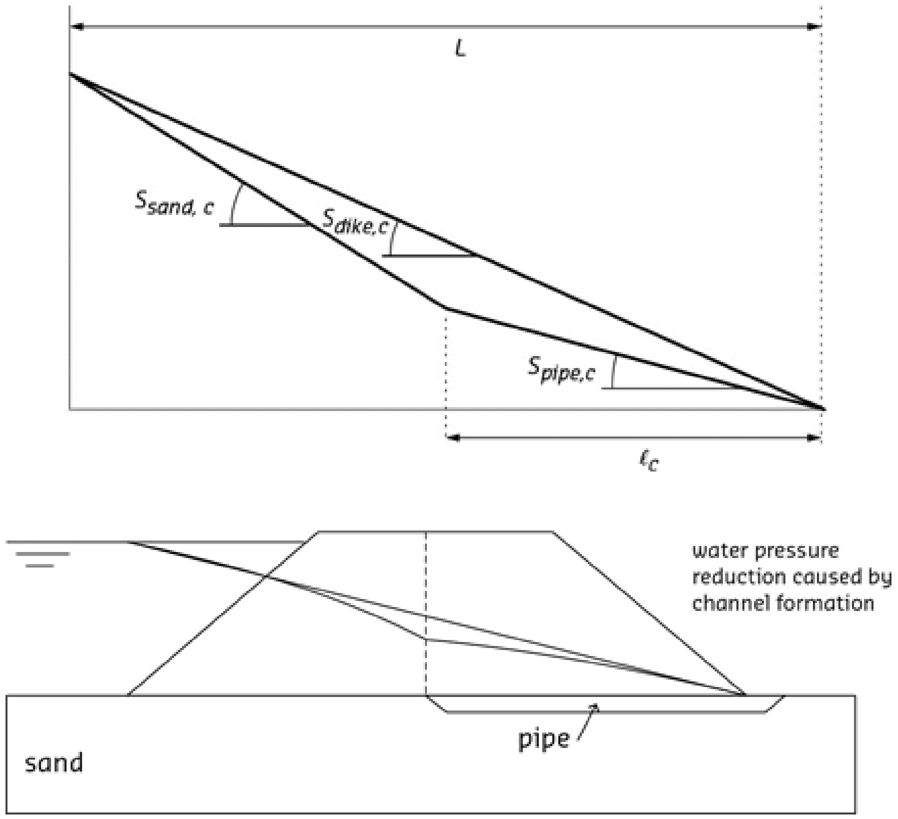

Figure 3: Schematization of critical hydraulic gradients

To obtain the critical gradient across the dike, three unknowns need to be determined, which are the critical average gradient upstream of the pipe $S_{sand,c}$, the critical pipe length ℓ_c and the critical pipe gradient $S_{pipe,c}$ (at which the particles are in limit-state equilibrium). Using the continuity equation in zone A (thus assuming that the flow through zone A is equal to the total flow through the pipe), the critical hydraulic gradient in the sand can be given by:

$$S_{sand,c} = S_{pipe,c} \frac{\Omega_{s,A,c}}{\Omega_{p,c}} \tag{14}$$

In this equation the 'resistance of the sand $\Omega_{s,A,c}$' is unknown. Therefore a 'virtual discharge' dQ* is introduced in zone B. The total flow through zone B, including the virtual discharge

$$Q_2^* = Q_2 + dQ^* \tag{15}$$

is assumed to be equal to $\frac{S_{pipe}}{\Omega_s}$. Using this equation, it can be derived that (for further explanation see Hoffmans, unpublished):

$$\Omega_{s,A,c} = \Omega_s + \Omega_{p,c} \quad \text{with } \Omega_s = (BDK)^{-1} \tag{16}$$

When this equation is combined with equation 14, the resulting equation for $S_{sand,c}$ is:

$$S_{sand,c} = \left(1 + \frac{\Omega_s}{\Omega_{p,c}}\right) S_{pipe,c} = S_{pipe,c} + Q_{p,m,c}\Omega_s = S_{pipe,c} + \frac{q_{p,m,c}}{DK} \tag{17}$$

Hence, the critical hydraulic dike gradient may be written as (see also Eq. 1):

$$\frac{H_c}{L} = S_{pipe,c} + \left(1 - \frac{\ell_c}{L}\right) \frac{q_{p,m,c}}{DK} \tag{18}$$

Noteworthy, but not required for the further analysis of the critical gradient is that the thickness of zone A can now be written based on the continuity equation ($Q_{1,A} = Q_{p,m}$) as:

$$D_{ref} = \frac{Q_{p,m}}{BKS_{sand}} = \frac{q_{p,m}}{KS_{sand}} \tag{19}$$

or with Equation 15:

$$D_{ref} = D\left(1 - \frac{S_{pipe}}{S_{sand}}\right) \tag{20}$$

The average gradient in the pipe, which is an unknown in equation 18 is based on the equilibrium of particles (Equation 5 and 10):

$$S_{pipe,c} = \frac{\Psi_{\ell am,c}(\rho_s/\rho - 1)d_{15}}{R_c} \tag{21}$$

Since the hydraulic radius is unknown Eq. 21 is rewritten by using equation 5 and the definition of the Reynolds number:

$$S_{pipe,c} = \frac{\sqrt{g}\left(\Psi_{\ell am,c}\left(\rho_s/\rho - 1\right)d_{15}\right)^{3/2}}{\nu\sqrt{\alpha_{\mathrm{Re},\ell}}} \tag{22}$$

where the calibration parameter $\alpha_{\mathrm{Re},\ell}$ is assumed to be a constant (Hoffmans and Van Rijn, 2017) and includes the variation in pipe height from upstream to downstream (through $C_{\ell,c} = \frac{\ell_{p,h,c}}{\ell_{p,m,c}}$) and the Reynolds number at the downstream side of the pipes.

$$\alpha_{\mathrm{Re},\ell} = \tfrac{1}{2}\left(1 + C_{\ell,c}\right)^2 \mathrm{Re}_{m,c} \tag{23}$$

The normalized critical pipe length is determined using Equation 24, which was based on the assumption that the critical pipe length depends on the shape of the aquifer (D/L) and the pipe gradient, using computational results of the Sellmeijer model. The factor α_f is a calibration factor:

$$\frac{\ell_c}{L} \approx \exp\left(-\left(\frac{\alpha_f D}{L}\right)^2 S_{pipe,c}\right) \tag{24}$$

The total flow through the pipe, $q_{p,m,c}$ can be rewritten using the Reynolds number in the pipe at the downstream side ($q_{p,m,c} = 2\,\mathrm{Re}_{m,c}\,\nu$). The Reynolds number ($\mathrm{Re}_{m,c}$) is not known, but is estimated based on the mean grain size and a calibration parameter ℓ_{Re}:

$$2\,\mathrm{Re}_{m,c} \approx \frac{d_{50}}{\ell_{\mathrm{Re}}} \tag{25}$$

This is justified as follows. The flow through the pipe and its shape depend on the flow towards the pipe. Consequently, the critical pipe dimensions (through $C_{\ell,c}$ giving the ratio of the pipe diameter at the exit point and the middle of the seepage path) are related to the relation between pipe resistance and sand resistance ($C_{G,v} = \Omega_p / \Omega_{s,A}$). If these assumptions are taken into account and applying equation 5 then (see also Hoffmans (unpublished) for a justification):

$$\frac{2\left(1 + C_{G,v}\right)C_{\ell,c}^4}{1 + C_{\ell,c}} = 1 \tag{26}$$

If the vertical groundwater can easily flow into the pipes (thus if $C_{G,v} \to \infty$ or if K is large) then the pipes are cone-shaped ($C_{\ell,c} \to 0$). If the vertical inflow is negligible (thus if $C_{G,v} \to 0$ or if K is small) then the pipe geometry does not alter ($C_{\ell,c} \to 1$). Using the Kozeny-Carman equation ($K \propto d^2$) the following approximation can be made (for $0_{|d = 0.5\text{ mm}} < C_{\ell,c} < 0.7_{|d = 0.2\text{ mm}}$).

$$\frac{1 + C_{\ell,c}}{d^{-1/2}} \approx \text{constant} \tag{27}$$

Since the summation of the vertical inflow increases from the entry points to the exit point the flow velocities and Reynolds numbers in the pipes increase. On the landside the critical Reynolds number is at maximum and is written as:

$$\mathrm{Re}_{m,c} = \frac{4\,\mathrm{Re}_c}{\left(1 + C_{\ell,c}\right)^2} \tag{28}$$

Hence,

$$2\,\mathrm{Re}_{m,c}\,\nu \approx \frac{d_{50}\nu}{\ell_{\mathrm{Re}}} \tag{29}$$

Note that according to the SD-model thick sand layers (say $D/L > 0.5$) are very unstable since the critical pipe length equals approximately nil. In such cases, the critical Shields parameter must be lowered from 'general transport' to 'no erosion' which results in a smaller allowable dike gradient.

2.5 Calibration

Both the Sellmeijer model and the SD model were calibrated to laboratory experiments. Sellmeijer's model was calibrated in different research periods. Shortly after the development of the initial rule (Sellmeijer et al., 1989), large scale experiments were conducted in the DeltaFlume (Silvis, 1991), using only one sand type. The bedding angle was calibrated to these experiments and based on expert judgment a value of 41 degrees was selected in combination with White's coefficient of 0.25 for prediction of piping in practice (TAW, 1999). After the numerical implementation of the Sellmeijer model in 2006, a bedding angle of 37 degrees was selected based on the same calibration (Sellmeijer, 2006). At the time it was initially presented, it was already realized that especially for coarse grained material the rule did not match well with experimental results (Weijers and Sellmeijer, 1993). A renewed calibration was conducted in 2011, after a series of small-, medium- and full-scale experiments (Van Beek et al., 2011). A multi-variate analysis was conducted on the results of small-scale experiments only, relating material properties like hydraulic conductivity, grain size (d70), uniformity coefficient and roundness to the critical head. From this analysis it was concluded that the effect of roundness was limited (although the tested selection of natural sands did not show a lot of variation in roundness), and the effect of grain size was smaller compared to the original Sellmeijer rule. Lacking a theoretical explanation, the rule was adjusted using the empirical factors obtained from the multi-variate analysis, while retaining the fitted bedding angle from the previous calibration. The empirical fitting leads to the clear disadvantage for the model of not being applicable outside the tested range of sand types.

The SD model counts three unknowns: a length scale parameter (l_{Re}), a groundwater coefficient (α_f) and a Reynolds coefficient ($\alpha_{Re,l}$). All available laboratory experiments (leaving out duplicates) from Dutch literature were used to calibrate and validate these three parameters.

Calibration of models with field or laboratory data is often inevitable. However, when extrapolating outside the calibration range, it is of importance to verify that the calibration parameters are really constants under all circumstances. The bedding angle, used as a calibration parameter in the Sellmeijer model is essentially not a constant, and results in overestimation of the critical shear stress for coarser sands (Van Beek et al., 2015), which required a correction through empirical factors. The length scale and geometric pipe coefficients in the SD model are a function of several parameters including the Reynolds number in the pipe, in turn dependent on the velocity and particle depth in the pipe. The consequence of keeping these two parameters constant for all circumstances is not investigated here, although the fit proves to be good for experiments at small and medium scale and Hoffmans and Van Rijn (2017) have verified these constants at differents scales.

2.6 Validation

After adaptation of the Sellmeijer rule with the empirical factors based on the small-scale experiments, the result was calibrated with the medium- and full-scale experiments (Sellmeijer et al., 2011). It was

$$\mathrm{Re}_{m,c} = \frac{4\,\mathrm{Re}_c}{\left(1 + C_{\ell,c}\right)^2} \tag{28}$$

Hence,

$$2\,\mathrm{Re}_{m,c}\,\nu \approx \frac{d_{50}\nu}{\ell_{\mathrm{Re}}} \tag{29}$$

Note that according to the SD-model thick sand layers (say $D/L > 0.5$) are very unstable since the critical pipe length equals approximately nil. In such cases, the critical Shields parameter must be lowered from ‘general transport’ to ‘no erosion’ which results in a smaller allowable dike gradient.

2.5 Calibration

Both the Sellmeijer model and the SD model were calibrated to laboratory experiments. Sellmeijer’s model was calibrated in different research periods. Shortly after the development of the initial rule (Sellmeijer et al., 1989), large scale experiments were conducted in the DeltaFlume (Silvis, 1991), using only one sand type. The bedding angle was calibrated to these experiments and based on expert judgment a value of 41 degrees was selected in combination with White’s coefficient of 0.25 for prediction of piping in practice (TAW, 1999). After the numerical implementation of the Sellmeijer model in 2006, a bedding angle of 37 degrees was selected based on the same calibration (Sellmeijer, 2006). At the time it was initially presented, it was already realized that especially for coarse grained material the rule did not match well with experimental results (Weijers and Sellmeijer, 1993). A renewed calibration was conducted in 2011, after a series of small-, medium- and full-scale experiments (Van Beek et al., 2011). A multi-variate analysis was conducted on the results of small-scale experiments only, relating material properties like hydraulic conductivity, grain size (d70), uniformity coefficient and roundness to the critical head. From this analysis it was concluded that the effect of roundness was limited (although the tested selection of natural sands did not show a lot of variation in roundness), and the effect of grain size was smaller compared to the original Sellmeijer rule. Lacking a theoretical explanation, the rule was adjusted using the empirical factors obtained from the multi-variate analysis, while retaining the fitted bedding angle from the previous calibration. The empirical fitting leads to the clear disadvantage for the model of not being applicable outside the tested range of sand types.

The SD model counts three unknowns: a length scale parameter (l_{Re}), a groundwater coefficient (α_f) and a Reynolds coefficient ($\alpha_{Re,l}$). All available laboratory experiments (leaving out duplicates) from Dutch literature were used to calibrate and validate these three parameters.

Calibration of models with field or laboratory data is often inevitable. However, when extrapolating outside the calibration range, it is of importance to verify that the calibration parameters are really constants under all circumstances. The bedding angle, used as a calibration parameter in the Sellmeijer model is essentially not a constant, and results in overestimation of the critical shear stress for coarser sands (Van Beek et al., 2015), which required a correction through empirical factors. The length scale and geometric pipe coefficients in the SD model are a function of several parameters including the Reynolds number in the pipe, in turn dependent on the velocity and particle depth in the pipe. The consequence of keeping these two parameters constant for all circumstances is not investigated here, although the fit proves to be good for experiments at small and medium scale and Hoffmans and Van Rijn (2017) have verified these constants at differents scales.

2.6 Validation

After adaptation of the Sellmeijer rule with the empirical factors based on the small-scale experiments, the result was calibrated with the medium- and full-scale experiments (Sellmeijer et al., 2011). It was found that the adapted rule performed better than the original rule, especially for coarser sand, for which the original rule was found to be unsafe.

The SD model was validated using basically the same set of experiments as for the calibration, by applying the duplicates of the tests. Next to this, the SD model is verified by using three Delta-flume experiments and three IJkdijk tests, for which the model predicts well. Finally the results of the SD model were compared to three field cases, one Chinese dike (failed dike) and two Dutch dikes (heavy sand boils). It should be realized that the input parameters of these field cases are rough estimates, and are therefore not very suitable for the precise validation of models. Next to this, many aspects that are known to affect the occurrence of piping are not yet included in the models, such as heterogeneity of the subsurface and 3D-flow, which also complicates the validation of models with field cases. Field cases can be used to compare general trends, but are not well suited for validation on an individual basis.

One general trend that is essential for the extrapolation to the field is the effect of scale on the critical gradient. Figure 4 shows the scale effect in different models resulting from increase of length, while retaining D/L ratio and sand characteristics (fine sand). It is noted here that due to the constant D/L ratio, the same trends can be found when using the aquifer thickness as reference scale. Figure 5 shows a similar graph with experimental and field data. Although obviously more parameters that influence the critical gradient are not plotted, causing scatter, a general decrease with increase of scale can be observed.

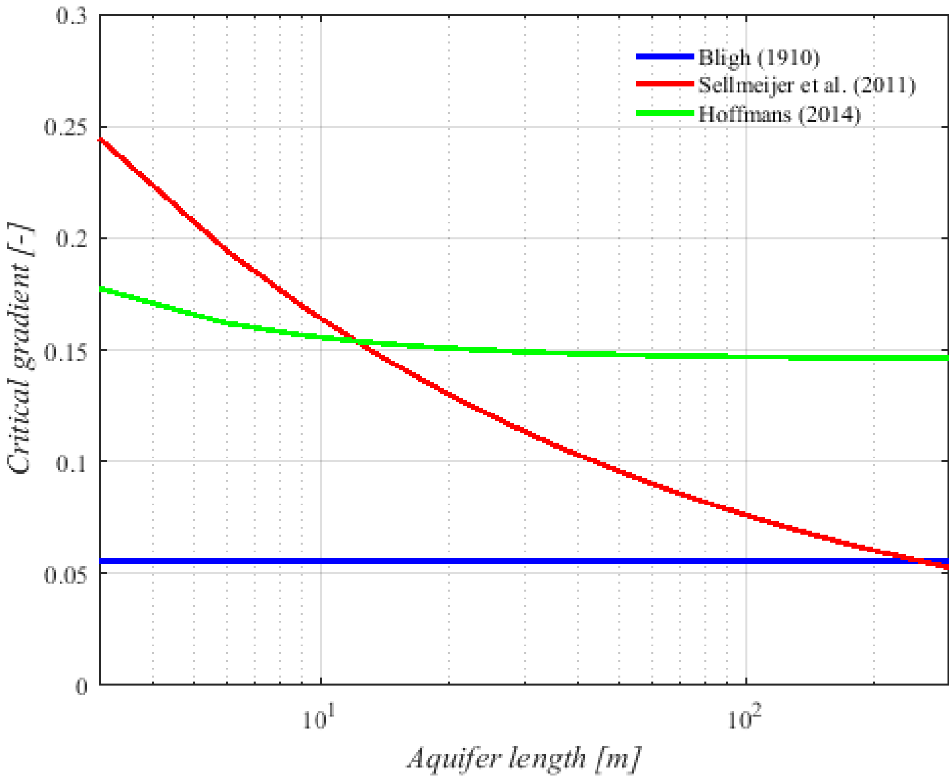

Figure 4. Illustration of the scale effect (represented by L) in different models, given a constant D/L ratio of 1/3 and constant material properties (fine sand)

Comparison of the graphs shows that a decrease of critical gradient with increase of scale is expected, but that the degree by which critical gradient decreases with scale significantly varies for the different models. The scale effects are much more limited in the SD model (and even absent once a certain aquifer depth is exceeded), compared to the Sellmeijer model, which converges to the rule of Bligh for the chosen configuration. It is noted that the recommendation for the SD model to move from ‘general transport’ to ‘no erosion’ is not followed for these cases since the D/L ratio is much smaller than 1. A possible cause for the difference in outcome is the inclusion of groundwater flow in deeper layers in the

Sellmeijer model, as opposed to the SD layer, in which it is assumed that flow through deeper layers does not affect the piping process. Next to this, the groundwater flow is simplified for the SD model, whereas it was numerically calculated for the Sellmeijer model (using MSEEP).

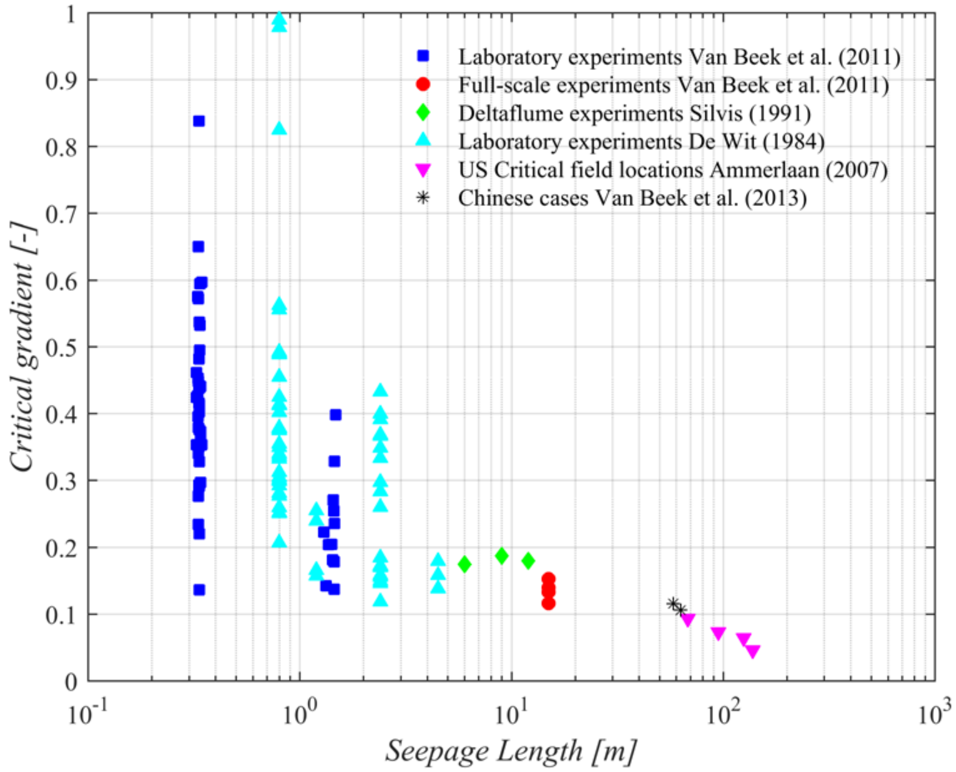

Figure 5. Illustration of the scale effect (as represented by L) in laboratory experiments and field data

3 A FUTURE PERSPECTIVE ON BACKWARD EROSION PIPING MODELLING

In the last years, a significant amount of research has been conducted to better understand the occurrence of backward erosion piping. The models discussed here, the Sellmeijer model and SD model both simplify reality. Since a model is always a simplification of reality, this is essentially not an issue. However, if effects are excluded or simplified that turn out to be of major importance to the outcome of the model, the model may become impractical or even incorrect. For example, recent research shows that the assumption of 2D flow may lead to unsafe predictions, whereas heterogeneity may lead to additional strength. Calibration with field cases may overcome this issue, as can be seen in the model of Lane (1935), which has a limited theoretical basis, but is generally considered as a safe method for design against backward erosion piping for structures with a vertical component in the seepage path, due to the numerous cases on which it relies. For backward erosion piping without vertical structures this is more difficult, since only a few failure cases are available and the relevant parameters are difficult to determine accurately. Sand boils indicate a susceptibility to piping, but are known to occur at lower water levels than the critical head and therefore do not give an indication of the critical head. Given the limited number of field cases, much depends on the extrapolation from laboratory results to the field, which requires a full understanding of the physical processes involved and the characteristics in the field. Once the physical processes are fully understood, a simplification of reality is still often requested and can be safe when conservative choices are made for schematization. An accumulation of conservative choices however, e.g. homogeneous subsurface, steady-state groundwater flow calculations, conservative input parameters, will result in a safe outcome, but this can also be impractical in the field due to the lack of distinction.

At this point several steps still need to be taken for reliable prediction of piping in practice, consisting of better characterization of the field situation, in terms of heterogeneity and groundwater flow, the collection of observations, a better understanding of the mechanism in various (heterogeneous) soil types, including the development of criteria for pipe lengthening, widening and deepening, and the modeling of the mechanism. Based on the current state of the art of backward erosion modelling, this will, among other things, involve 3D modeling of the process, including the expected variability of the sand layer, and validation with full-scale field tests. Calculation rules based on simplified schematizations may still be useful in an early stage of a safety assessment, if the physical processes are well enough understood to extrapolate to the field.

Considering this, aspects of the Sellmeijer model and SD model will likely still be found in the future developments, such as the Shields approach (not only in laminar but also in turbulent conditions) for prediction of the head loss in the pipe, the pipe flow through shallow and wide pipes and the groundwater flow towards the pipe (numerically calculated, allowing for complex configurations).

4 CONCLUSIONS AND RECOMMENDATIONS

This paper evaluates two Dutch backward erosion piping models, the Sellmeijer model and the SD model. The models are rather similar, since both rely on erosion criteria which are driven by 2D groundwater flow and laminar flow through the pipe. Although the models are similar, the outcomes of the models are very different, especially for prototype conditions.

The SD model simplifies the groundwater flow, by assuming zones in the subsurface where the head drop changes linearly. In the Sellmeijer model the flow towards the pipe is calculated numerically in MSEEP. Recent investigations (Vandenboer et al. (2014a and 2014b), Van Beek et al. (2015),) indicate the importance of 3D groundwater flow calculations. Models calibrated with experiments with 2D exits and limited width may overestimate the critical gradient, leading to an unsafe result.

Erosion criteria control the progression of the pipe. The Sellmeijer model relies on erosion in the pipe only, using a particle equilibrium based on the approach by White (1940), with a constant value for the bedding angle calibrated in large-scale experiments, whereas in the SD model the more widely accepted Shields approach is applied. Recent experiments indicate the existence and relevance of a local, scale-independent critical gradient upstream of the pipe, which is currently not included in the models.

Both models have several calibration parameters, although the used set of experiments for calibration differs. The SD model was calibrated with an extensive set of laboratory experiments and validated with the duplicate experiments of this set, whereas the Sellmeijer model was calibrated with one series of small-scale experiments and validated with medium- and full-scale experiments. The SD model was verified with six large scale experiments and compared with some field cases. Here it is noted that field cases can be used for validation of general trends, but single cases cannot be easily used for validation of models. Extrapolation of the models to the field therefore remains challenging. Based on available experiments and cases it can be concluded that considerable scale effects exists.

The two models as discussed have been calibrated and validated with tests on a small, medium and a large scale. They both yield satisfactory results for the experiments that have been investigated. However, for prototype conditions large differences occur, which are likely related to the manner of groundwater flow calculation. In addition, important aspects like 3D flow, heterogeneity and time dependency are currently not included in the assessment rules, although the Sellmeijer model implemented in DGFlow (Van Esch et al., 2013) already offers far more possibilities than the rules. Future developments should aim for an improved piping model, which include aspects of both models, such as the Shields approach for prediction of the head loss in the pipe, the pipe flow through shallow and wide pipes and the numerical calculation of groundwater flow towards the pipe, combined with new insights on a local, scale-independent criterion for progression at the pipe tip. In addition better subsurface characterization and collection of field observations are essential for model validation and safety assessment.

LIST OF NOTATIONS

B	width of the dike (m)
$C_{G,v}$	vertical seepage transmissivity (-)
C_ℓ	geometry factor of pipe (-)
d	particle diameter (m)
d_i	particle diameter for which i% of the sediment particles is finer than d_i (m)
D	thickness of the sand layer (m)
D_{ref}	(= D_{eff}) thickness of zone A (below the pipes) (m)
D_*	[= $d_{50}(\Delta g/\nu^2)^{1/3}$] dimensionless particle diameter related to d_{50} (-)
g	acceleration due to gravity (m/s^2)
H	local head (m)
H_1	river level (m)
H_2	water level in the ditch or surface level (m)
H_ℓ	hydraulic head where erosion in the pipe starts (m)
K	hydraulic conductivity of sand layer (m/s)
ℓ	length of pipe (m)
ℓ_{Re}	(= $18\cdot10^{-6}$ m) length scale (m)
L	seepage length (m)
q	discharge per unit width, outflow (m^2/s)
Q	discharge (m^3/s)
Q_1	(= $Q_{1,A} + Q_{1,B}$) discharge in sand layer at the inflow section (riverside) (m^3/s)
Q_2	discharge in sand layer at outflow section (landside) (m^3/s)
RD	packing density (-)
RD_m	(= 0.725; default value) packing density (-)
Re	Reynolds pipe number (-)
Re_m	Reynolds pipe number on the landside (at $x = 0$) (-)
R	hydraulic radius (m)
S	average hydraulic gradient (-)
S_{dike}	average hydraulic dike gradient (-)
S_{pipe}	hydraulic pipe gradient (mean hydraulic gradient in the pipes) (-)
S_{sand}	hydraulic sand gradient (mean hydraulic gradient upstream of the pipes) (-)
S_{vert}	hydraulic vertical gradient (in zone A) (-)
α_f	(= 5) groundwater coefficient (-)
$\alpha_{\mathrm{Re},\ell}$	(= 6) geometric pipe coefficient (-)
γ'_p	under water particle weight (N/m^3)
Δ	(= $\rho_s/\rho_w - 1$) relative particle density (-)
η	White coefficient (-)
κ	(= $K\nu/g$) intrinsic permeability (m^2)
ν	kinematic viscosity (m^2/s)
ρ	density of water (kg/m^3)
ρ_s	density of particles (kg/m^3)
τ_c	critical mean wall shear stress (N/m^2)
$\tau_{c,k}$	critical characteristic wall shear stress (N/m^2)
τ_w	mean wall shear stress (N/m^2)
Ψ	Shields parameter (-)
Ω	resistance of conductor (ohms)
Ω_p	pipe or overall pipe resistance (s/m^3)
$\Omega_{p,h}$	horizontal pipe resistance (s/m^3)

Ω_s	horizontal seepage resistance (s/m^3)
$\Omega_{s,A}$	horizontal seepage resistance in zone A (s/m^3)
$\Omega_{s,B}$	horizontal seepage resistance in zone B (s/m^3)
$\Omega_{s,h}$	horizontal seepage resistance in zone A (s/m^3)
$\Omega_{s,v}$	vertical seepage resistance in zone A (s/m^3)

Subscripts

c	critical
ℓam	laminar

REFERENCES

Ammerlaan, P.R.M. (2007). *Levees and levee evaluation – The Dutch and US practice compared*. Msc. Thesis, TU Delft.

Bligh, W.G. (1910). Dams Barrages and Weirs on Porous Foundations. *Engineering News* 64(26): 708-710.

De Wit, J.M. (1984) *Onderzoek zandmeevoerende wellen Rapportage Modelproeven*. Grondmechanica Delft report CO-220887/10.

Ding, L., Yao, Q., Sun D., Liu, C. (2007). Experimental studies on piping development in three-stratum dike foundations. *Water Resources and Hydropower Engineering*, 38(2): 19-22.

Govers, G. (1987). Initiation of motion in overland flow. *Sedimentology* 34:1157-1164.

Grass, A.J., 1970. Initial instability of fine bed sand, Hydraulic Division, *Proc. of ASCE*, Vol. 96, HY3, pp. 619-632.

Hanses, U. (1985). *Zur Mechanik der Entwicklung von Erosionskanälen in geschichtetem Untergrund unter Stauanlagen*. Dissertation Grundbauinstitut der Technischen Universität Berlin, Germany.

Harza, L.F. (1935). Uplift and seepage under dams on sand. *Transactions American Society of Civil Engineers* 100: 1353-1406

Hoffmans, G.J.C.M., 2014. An overview of piping models. Keynote Lecture. *Proc. of Int. Symp. of Scour and Erosion*. Perth, Australia.

Hoffmans, G.J.C.M., Van Rijn, L.C. (2017). Hydraulic approach for predicting piping in dikes. *Journal of Hydraulic Research*, ISSN 0022-1686 print/ISSN 1814-2079 online: http://www.tandfonline.com

Hoffmans, G.J.C.M. (upublished). *Shields-Darcy model. Alternative piping model?* – available upon request.

Kanning, W. (2012). *The Weakest Link – Length Effects for Piping*. Phd thesis, Delft University of Technology, Delft, The Netherlands.

Lane, E.W. (1935). Security from under-seepage masonry dams on earth foundations. *Transactions American Society of Civil Engineers* 100:1235-1351.

Loiseleux, T., Gondret, P., Rabaud, M., Doppler D. (2005). Onset of erosion and avalanche for an inclined granular bed sheared by a continuous laminar flow. Physics of fluids 17(103304): 1-9.

Müller-Kirchenbauer, H. (1978). Zum Zeitlichen Verlauf der Rückschreitenden Erosion in Geschichtetem Untergrund unter Dämmen und Stauanlagen, Beitrag zum *Talsperrensymposium*, München.

Navin, M. (2016). Kaskaskia Island and Bois Brule Levee Breaches during the 1993 Mississippi River Flood. *International Symposium on the Mechanics of Internal Erosion for Dams and Levees*.

Pilotti, M. and Menduni, G., 2001. Beginning of sediment transport of incoherent grains in shallow shear flows. *Journal of Hydraulic Research*, Vol. 39, No. 2, p. 115-124.

Robbins, B.A. (2016). Numerical modeling of backward erosion piping. *Applied Numerical Modeling in Geomechanics*, eds Gómez, Detournay, Hart and Nelson (eds.). p. 551-558.

Robbins, B.A., Van Beek, V.M., López – Soto, J.F., Montalvo-Bartolomei, A.M., Murphy, J. (to be published). A novel laboratory test for backward erosion piping. *International Journal of Physical Modelling in Geotechnics*.

Robbins, B.A. and Van Beek, V.M. (2017). Physical measurements of the backward erosion piping process. *Proceedings 25th meeting European Working Group on Internal Erosion*.

Rotunno, A.F., Callari, C., Froiio, F. (2017). Computational Modeling of Backward Erosion Piping. Models, *Simulation, and Experimental Issues in Structural Mechanics*, Springer Series in Solid and Structural Mechanics 8, M. Frémond et al. (eds.), Springer International Publishing DOI 10.1007/978-3-319-48884-4_12.

Sellmeijer, J.B. (2006). Numerical computation of seepage erosion below dams (piping). In *Proceedings Third International Conference on Scour and Erosion*, 596-601, CURNET, Gouda, The Netherlands.
Sellmeijer, J.B. (1988). *On the mechanism of piping under impervious structures*. Doctoral dissertation, TU Delft, The Netherlands.
Sellmeijer, J.B., Calle, E.O.F., Sip, J.W. (1989). Influence of aquifer thickness on piping below dikes and dams. *In Proceedings of International symposium on analytical evaluation of dam related safety problems*, 357-366.
Sellmeijer J.B., Lopéz de la Cruz J., Van Beek V.M., Knoeff J.G. (2011). Fine-tuning of the piping model through small-scale, medium-scale and IJkdijk experiments. *European Journal of Environmental and Civil Engineering* 15(8): 1139-1154.
Shields, A. (1936). *Anwendung der Ahnlichkeitsmechanik und Turbulenzforschung auf die Geschiebebewegung*. Mitteilungen der Preuβischen Versuchsanstalt für Wasserbau und Schiffbau, heft 26, Berlin.
Silvis, F. (1991). *Verificatie Piping Model: Proeven in de Deltagoot. Grondmechanica Delft*, Delft, The Netherlands.
TAW (1999). *Technisch rapport Zandmeevoerende wellen*. Technische Adviescommissie voor de Waterkeringen, Delft, The Netherlands.
Van Beek, V.M., Knoeff, J.G., Sellmeijer, J.B. (2011). Observations on the process of backward piping by underseepage in cohesionless soils in small-, medium- and full-scale experiments. *European Journal of Environmental and Civil Engineering* 15(8): 1115-1137.
Van Beek, V.M., Bezuijen A., Sellmeijer, J.B., Barends F.B.J. (2014). Initiation of backward erosion piping in uniform sands, *Géotechnique* 64(12): 927-941.
Van Beek, V.M., Van Essen, H.M., Vandenboer, K., Bezuijen, A. (2015). Developments in modelling of backward erosion piping. *Géotechnique* 65(9): 740-754.
Van Beek, V. M., Yao, Q.L., Van, M.A., 2013. Backward Erosion piping model verification using cases in China and the Netherlands, Paper No. 3.29a, *7th Int. Conf. on Case Histories in Geotechnical Engineering and Symposium in Honor of Clyde Baker*.
Van Beek, V., Yao Q., Van M., Barends F. (2012). Validation of Sellmeijer's model for backward piping under dikes on multiple sand layers, *Proceedings of 6th International Conference on Scour and Erosion*, pp. 543-550.
Van Esch, J.M., Sellmeijer, J.B., Stolle, D. (2013). Modeling transient groundwater flow and piping under dikes and dams. *Proceedings COMGEO III*, Krakow, Poland, International Centre for Computational Engineering.
Van Rijn, L.C., 2014. *Review of Piping Processes and Models*, Report prepared for Deltares. www.leovanrijn-sediment.com.
Vandenboer, K., Van Beek, V., Bezuijen, A. (2014a). 3D finite element method (FEM) simulation of groundwater flow during backward erosion piping. *Front. Struct. Civ. Eng.* 8(2): 160 – 166.
Vandenboer, K, Bezuijen, A, Van Beek, VM (2014b). 3D character of backward erosion piping: Small-scale experiments. In Scour and Erosion (Cheng, Draper and An (Eds)), *Scour and Erosion*, p. 81-86, Taylor & Francis Group, London.
Vrijling, J.K., Kok, M., Calle, E.O.F., Epema, W.G., Van der Meer, M.T., Van den Berg, P., Schweckendiek, T. (2010). Piping - *Realiteit of Rekenfout?* Technical report, Dutch Expertise Network on Flood Protection (ENW).
Vrijling, JK; Schweckendiek, T; Kanning, W. (2011b). Safety standards of flood defenses. *Proceedings of the 3rd International Symposium on Geotechnical Safety and Risk*, ISGSR 2011. ed. N Vogt; B Schuppener; D Straub; G Brau. p. 67-84.
Weijers, J.B.A. and Sellmeijer, J.B. (1993). A new model to deal with the piping mechanism. In *Filters in Geotechnical and Hydraulic Engineering* (Brauns, Schuler and Heibaum (eds)) 349-355, Balkema, Rotterdam, the Netherlands.
White, C.M. (1940). The equilibrium of grains on the bed of a stream. *Proceedings Royal Society*, no. 174A, p. 322-338.